Z^0 production in TeV neutrino and antineutrino scattering off nucleons

R. Bates
Okanagan College, 1000 KLO Road, Kelowna, British Columbia, Canada V1Y 4X8

John N. Ng
TRIUMF Theory Group, 4004 Wesbrook Mall, Vancouver, British Columbia, Canada V6T 2A3

(Received 15 September 1989)

We calculated the production cross section of the Z^0 boson in multi-TeV ν and $\bar{\nu}$ scattering off nucleons in the standard model. The production cross section from $\bar{\nu}$ is found to be larger than that of ν. At $E_\nu = 20$ TeV the production rate is 10^{-4} pb. A detailed energy dependence of the production rate and the angular dependence of outgoing muons and the Z^0 are given.

I. INTRODUCTION

In this paper we study the production of Z^0 bosons in very-high-energy neutrino (antineutrino) collisions with nucleons. In particular, the semi-inclusive reactions investigated are

$$\nu_\mu N \to \mu^- Z^0 X \ , \tag{1.1a}$$

$$\bar{\nu}_\mu N \to \mu^+ Z^0 X \ , \tag{1.1b}$$

where X denotes any hadronic states and N is a nucleon. We shall assume the quark-parton model for the collisions in Eq. (1.1). The dominant lepton-quark scattering subprocesses are

$$\nu_\mu(p_1)+d(p_2)\to\mu^-(p_3)+u(p_4)+Z^0(p_5) \ , \tag{1.2a}$$

$$\bar{\nu}_\mu(p_1)+u(p_2)\to\mu^+(p_3)+d(p_4)+Z^0(p_5) \ , \tag{1.2b}$$

where the four-momenta of the various particles given in their respective parentheses. The sea-quark contributions are unimportant. The Feynman diagrams depicting the reactions of Eq. (1.2) are given in Fig. 1.

The motivation for studying Z^0 in high-energy ν and $\bar{\nu}$ scattering is to test the three-gauge-boson coupling: namely, $Z^0W^+W^-$. In Z^0-boson production via Eq. (1.1) the only triple-gauge-boson coupling involved is $Z^0W^+W^-$. This is to be contrasted with $e^+e^-\to W^+W^-$ where both γW^+W^- and $Z^0W^+W^-$ couplings enter.[1] To test the standard-model one needs independent measurements of the γW^+W^- and $Z^0W^+W^-$ couplings. We know of one other process that measures the $Z^0W^+W^-$ coupling. This is the β decay of the $Z^0\to W^+l^-\bar{\nu}_l$ $(W^-l^+\nu_l)$ $l=e,\mu,\tau$. The branching ratio is calculated to be 3×10^{-8} in the standard model.[2] The smallness of the rate will require a high-intensity Z^0 factory. On the other hand, the strength of the γW^+W^- coupling can be measured in a variety of reactions[3,4] such as $p\bar{p}\to\gamma WX$, and $\gamma e^-\to W^-\nu$. Stringent tests of the standard-model triple-gauge-boson couplings will require doing at least three of the above-mentioned experiments.

To observe the reactions of Eq. (1.1) in the laboratory one will require neutrino beams with energy higher than 5 TeV. These will be available at the Superconducting Super Collider[5] (SSC) but not at the proposed Large Hardon Collider (LHC) at CERN.

Previous discussions of gauge-boson productions from lepton-proton collisions centered around electron-proton collisions.[6] This is partly due to the construction of HERA at DESY and the possibility of an ep option in

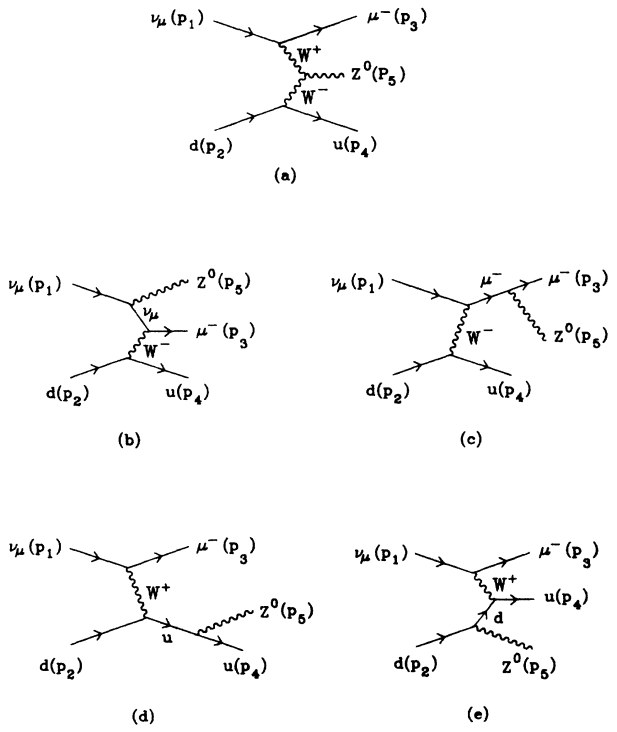

FIG. 1. Feynman diagrams for Z^0-boson production in the reaction $\nu_\mu d\to\mu^- uZ^0$. (a) t-channel W-boson exchange, (b) neutrino bremsstrahlung, (c) muon bremsstrahlung, (d) outgoing quark bremsstrahlung, (e) incoming quark bremsstrahlung.

both SSC and LHC. Earlier work on leptoproduction of gauge bosons is given in Ref. 7. As far as we can determine, reactions (1.1a), (1.1b) within the standard model have not been studied before and hence our work complements these previous studies.

In this paper we will be concerned only with the standard-model $Z^0W^+W^-$ vertex which is explicitly given by

$$\Gamma_{\mu\nu\lambda} = -ig\cos\theta_W[(p_1-p_2)_\lambda g_{\mu\nu}+(p_2-p_3)_\mu g_{\nu\lambda} +(p_3-p_1)_\nu g_{\lambda\mu}],$$

where p_1, p_2, p_3 denote the momenta of the Z^0, W^+, and W^- bosons, respectively. Previous calculations of the anomalous magnetic moment of the W boson in charged-Higgs-boson and supersymmetric models[8] and heavy-fermion models[9] showed that corrections to the standard-model values are small. We expect the same to hold for the $Z^0W^+W^-$ vertex in these renormalizable gauge models. Nonrenormalizable models such as composite models can give rise to much larger corrections. However, these are beyond the scope of this paper.

The calculation of the production rate of Eq. (1.1) is straightforward within the quark-parton model. We have used the spinor techniques of Ref. 10 as well as doing the square of the matrix element using the standard trace technique. We have checked the answers of the two calculations numerically and they agree with each other. In Sec. II we give details of the calculation. The phase-space integration is done by Monte Carlo integration. Section III contains our conclusions. In the Appendix we collect the relevant formulas for calculating the matrix element of Eq. (1.1) within the framework of the spinor technique.

II. CALCULATIONS AND RESULTS

The cross sections for the subprocesses $\nu_\mu d \to \mu^- Z^0 u$ and $\bar{\nu}_\mu u \to \mu^+ Z^0 d$ were obtained using standard techniques. The Feynman diagrams depicting the neutrino reaction are shown in Fig. 1. The antineutrino reaction proceeds via the same diagrams, but with the roles of the u and d quarks reversed. All fermion masses can be neglected at these energies.

The Feynman amplitudes were first calculated in a two-component-spinor basis for fermions, and left in complex form. The matrix element squared was then evaluated numerically using complex arithmetic. This method has the advantage of minimizing the algebraic manipulations done by hand. The details of the technique we used are described at length in Ref. 10. Our results are given in the Appendix.

In a separate calculation, the matrix element squared was also found using the traditional method of evaluating traces. The results were the same with those found using the spinor technique. The general expression obtained by the trace method is too lengthy to present here, but can be supplied upon request.

The quark-parton model was then used to estimate the cross sections for the physical processes of Eq. (1.1).

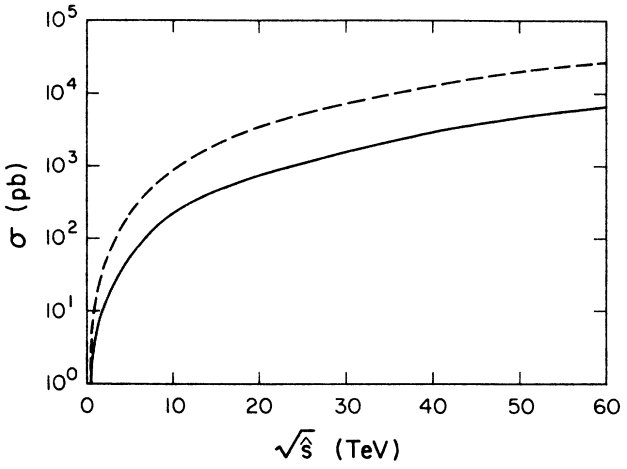

FIG. 2. Subprocess cross sections as a function of $\sqrt{\hat{s}}$. The solid line is for $\nu_\mu d \to \mu^- u Z^0$. The broken line is for $\bar{\nu}_\mu u \to \mu^+ d Z^0$.

Only the dominant valence quarks were considered. The subprocess cross sections were convoluted over the quark distribution functions in the manner of Eichten-Hinchliffe-Lane-Quigg[11] (EHLQ). Both the phase-space and convolution integrations were performed numerically using the Monte Carlo method. Good convergence was found in all cases. The cross sections as a function of the center-of-mass energy $\sqrt{s}$ are shown in Figs. 2 and 3. Values of the cross section near threshold for Z^0 production are given in Table I. It can be seen that antineutrino scattering generally produces more Z^0 bosons than neutrino scattering. Note however that the two values are comparable at $\sqrt{s}=200$ GeV, to within the accuracy of the Monte Carlo integration. This energy roughly corresponds to a 20-TeV neutrino (antineutrino) beam in the laboratory frame, for fixed target scattering. It is also

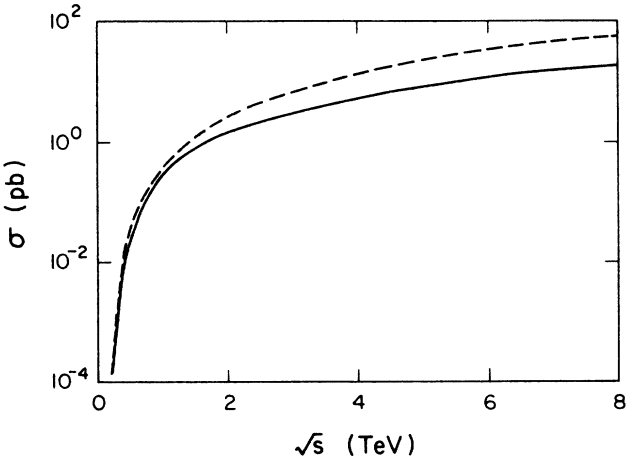

FIG. 3. Production cross sections as a function of $\sqrt{s}$. The solid line is for $\nu_\mu p \to \mu^- Z^0 X$. The broken line is for $\bar{\nu}_\mu p \to \mu^+ Z^0 X$.

TABLE I. Total neutrino (σ_ν) and antineutrino ($\sigma_{\bar\nu}$) cross sections near the Z^0-boson production threshold for 5-, 10-, 20-TeV neutrino (antineutrino) beams.

E_ν ($E_{\bar\nu}$) (TeV)	$\sqrt{s}$ (GeV)	σ_ν (pb)	$\sigma_{\bar\nu}$ (pb)
5	100	1.82×10^{-13}	1.19×10^{-11}
10	141	7.04×10^{-7}	1.85×10^{-6}
20	200	1.41×10^{-4}	1.36×10^{-4}

seen that even at the SSC the production cross section is 10^{-40} cm^2 on the nucleon. However, it is rising rapidly. At $\sqrt{s}=1$ TeV corresponding to $E_\nu=500$ TeV, the cross section is of the order of a picobarn. It appears that in the foreseeable future one will have to deal with production cross sections in the 10^{-40}-cm^2 range in the laboratory. For ultrahigh-energy neutrinos with $E_\nu=3.2\times10^7$ GeV (i.e., $\sqrt{s}=8$ TeV), such as would be expected from astrophysical sources, the Z^0 production is 5×10^{-35} cm^2. This is to be compared with the deep-inelastic cross section of $\nu_\mu N\to\mu^- X$ which is calculated[12] to be 2.3×10^{-34} cm^2.

Next, we examined the results for $\sqrt{s}=200$ GeV in more detail. As can be seen in Fig. 4, the Z^0 boson is produced with significant momentum for both the neutrino and antineutrino cases. The angular separation of the muon (antimuon) and the Z^0 boson in the center-of-mass frame for neutrino (antineutrino) scattering is shown in Fig. 5. The separations are large, and they differ in that there is a stronger tendency to favor a back-to-back configuration in the neutrino case. The other major difference was in the angular distribution of the muon (antimuon) itself. At this energy, we found the muon distribution was mostly isotropic with some bias towards the direction of the incoming neutrino. In contrast, the antimuon was mostly aligned with the direction of the incoming antineutrino.

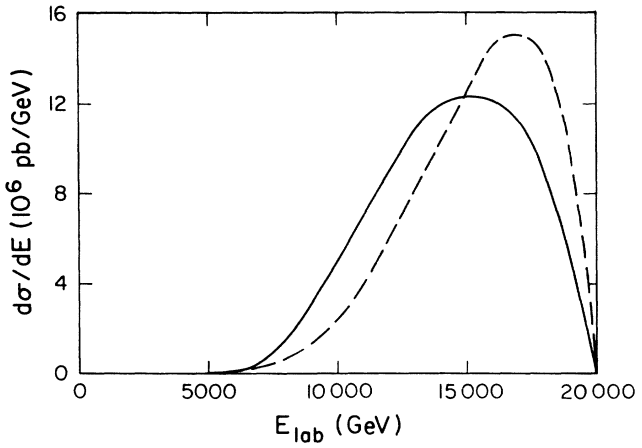

FIG. 4. Z^0-boson energy distribution in the laboratory frame with $\sqrt{s}=200$ GeV. The solid line is for $\nu_\mu p\to\mu^- Z^0 X$. The broken line is for $\bar\nu_\mu p\to\mu^+ Z^0 X$.

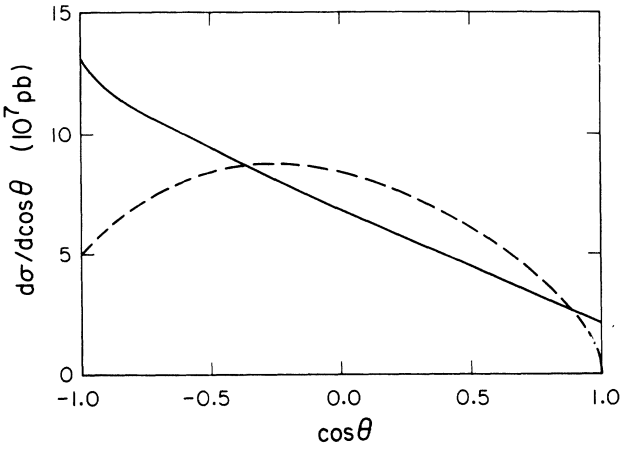

FIG. 5. Angular separation of the Z^0 boson and the muon in the c.m. frame with $\sqrt{s}=200$ GeV. The solid line is for $\nu_\mu p\to\mu^- Z^0 X$. The broken line is for $\bar\nu_\mu p\to\mu^+ Z^0 X$.

At energies far above threshold, these differences no longer occur. Both the muon (antimuon) and the Z^0 boson are strongly aligned with the direction of the incoming neutrino (antineutrino). This is to be expected since the neutrino (antineutrino) bremsstrahlung diagram has the largest coupling, and should dominate at high energy. The only remaining difference is that antineutrino scattering produces larger cross sections at these higher energies. As expected when boosted into the laboratory frame these opening angles become very small. Practically all the events accumulate in the bin $0.99\le\cos\theta\le1$.

III. DISCUSSION

We have calculated the production cross sections of the Z^0 boson for TeV ν and $\bar\nu$ scattering on protons and found them to be unobservably small near threshold energy of $E_\nu=5$ TeV, but is rising rapidly with E_ν. At $E_\nu=20$ TeV, the production cross is 10^{-4} pb. They level off around $E_\nu\sim10^6$ TeV. In general the antineutrino cross section is higher than that of the neutrino, partly due to the fact that there are two d quarks to scatter off for $\bar\nu$ compared with one u quark available in the ν case.

It is interesting to examine the ultrahigh-energy case, i.e., E_ν between 10^7–10^{10} GeV. Ultrahigh-energy (UHE) neutrinos are expected from astrophysical sources and can be looked for in the Fly's Eye and DUMAND detectors. The deep-inelastic $\nu_\mu N\to\mu^- X$ scattering cross section has been calculated[12] to be in the range of 10^{-33} and 10^{-32} cm^2 for E_ν between 10^7 and 10^9 GeV. Our results of Sec. II indicate that the Z^0 boson is about 3–5% of this for these UHE neutrinos. This can be understood in terms of the SU(2) gauge coupling g. The deep-inelastic cross section is of order g^4 whereas the Z^0 production cross section is of order g^6. The latter is suppressed by g^2 which is about 10%. Both cross sections rise logarithmically as a function of E_ν. The production of Z^0 will give rise to $\mu^+\mu^-$ and $\tau^+\tau^-$ pairs from the lepton decays of the Z^0. In addition, $Z^0\to b\bar b, c\bar c$ decay followed by the

semileptonic decays of the heavy quarks will also give rise to muon pairs. Hence, the muon content of these events will be mostly trimuons.

Our calculation can be easily extended to muon scattering on nucleons. One would expect the cross section for Z^0 production via $\mu^+ N \to \bar{\nu} Z^0 X$ to be the same order as in the neutrino case. Also for the SSC the muon flux is expected to be higher than the neutrino flux. At $E_\mu = 20$ TeV we find that $\sigma_{\mu^+ N} = 1.8 \times 10^{-4}$ pb for muon production; whereas $\sigma_{\nu N} \simeq \sigma_{\bar{\nu} N} \simeq 1.4 \times 10^{-4}$ pb (see Table I). Since the cross sections we are discussing are in the 10^{-4} pb range at the SSC, one would have to construct multikiloton detectors for this purpose. The alternative is to build higher-flux neutrino and/or muon beams.

ACKNOWLEDGMENTS

This work was partially supported by the Natural Sciences and Engineering Research Council of Canada.

APPENDIX: FEYNMAN AMPLITUDES

The amplitudes were calculated with Feynman rules in a two-component spinor basis. The techniques and notation we used are the same as those described in Ref. 8. For the neutrino subprocesses of Eq. (1.2a), the results are given in Eqs. (A1)–(A5). These correspond to the diagrams in Fig. 1:

$$m_a^\nu = -2F \cos^2\theta_W [(p_1-p_3)^2 - M_W^2]^{-1} [(p_2-p_4)^2 - M_W^2]^{-1}$$
$$\times \{ -S(p_3,\epsilon^*(p_5),p_1)^{--} S(p_4,p_5,p_2)^{--} + S(p_3,p_5,p_1)^{--} S(p_4,\epsilon^*(p_5),p_2)^{--}$$
$$+ 2[(p_4-p_2)\cdot\epsilon^*(p_5)][S(p_3,p_1)^{--} S(p_4,p_2)^{--} - S(p_3,p_2)^{--} S(p_4,p_1)^{--}] \} , \quad \text{(A1)}$$

$$m_b^\nu = -F[(p_2-p_4)^2 - M_W^2]^{-1} [(p_1-p_5)^2]^{-1}$$
$$\times [S(p_3,p_1-p_5,\epsilon^*(p_5),p_1)^{+}_{--} S(p_4,p_2)^{--} - S(p_3,p_2)^{--} S(p_4,p_1-p_5,\epsilon^*(p_5),p_1)^{+}_{--}] , \quad \text{(A2)}$$

$$m_c^\nu = -2F \sin^2\theta_W [(p_2-p_4)^2 - M_W^2]^{-1} [(p_3+p_5)^2]^{-1}$$
$$\times [S(p_3,\epsilon^*(p_5),p_3+p_5,p_1)^{--} S(p_4,p_2)^{--} - S(p_4,p_1)^{--} S(p_3,\epsilon^*(p_5),p_3+p_5,p_2)^{--}] , \quad \text{(A3)}$$

$$m_d^\nu = -F(1-\tfrac{4}{3}\sin^2\theta_W)[(p_1-p_3)^2 - M_W^2]^{-1} [(p_4+p_5)^2]^{-1}$$
$$\times [S(p_3,p_1)^{--} S(p_4,\epsilon^*(p_5),p_4+p_5,p_2)^{--} - S(p_3,p_2)^{--} S(p_4,\epsilon^*(p_5),p_4+p_5,p_1)^{--}] , \quad \text{(A4)}$$

$$m_e^\nu = -F(-1+\tfrac{2}{3}\sin^2\theta_W)[(p_1-p_3)^2 - M_W^2]^{-1} [(p_2-p_5)^2]^{-1}$$
$$\times [S(p_3,p_1)^{--} S(p_4,p_2-p_5,\epsilon^*(p_5),p_2)^{+}_{--} - S(p_4,p_1)^{--} S(p_3,p_2-p_5,\epsilon^*(p_5),p_2)^{+}_{--}] , \quad \text{(A5)}$$

where $\epsilon(p_5)$ is the polarization vector of the Z^0 boson, and

$$F = \frac{g^3 V_{ud}}{2\cos\theta_W} \omega_+(p_1)\omega_+(p_2)\omega_+(p_3)\omega_+(p_4) , \quad \text{(A6)}$$

where $V_{ud} = \cos\theta_C$ and θ_C is the Cabibbo angle. The quantities $\omega_+(p)$, $S(a,b)$, $S(a,b,c)$, and $S(a,b,c,d)$ are all defined in Ref. 10. For the antineutrino subprocess of Eq. (1.2b), the amplitudes are given in Eqs. (A7)–(A11):

$$m_a^{\bar{\nu}} = 2F \cos^2\theta_W [(p_1-p_3)^2 - M_W^2]^{-1} [(p_2-p_4)^2 - M_W^2]^{-1}$$
$$\times \{ -S(p_1,\epsilon^*(p_5),p_3)^{--} S(p_4,p_5,p_2)^{--} + S(p_1,p_5,p_3)^{--} S(p_4,\epsilon^*(p_5),p_2)^{--}$$
$$+ 2[(p_4-p_2)\cdot\epsilon^*(p_5)][S(p_1,p_3)^{--} S(p_4,p_2)^{--} - S(p_1,p_2)^{--} S(p_4,p_3)^{--}] \} , \quad \text{(A7)}$$

$$m_b^{\bar{\nu}} = -F[(p_2-p_4)^2 - M_W^2]^{-1} [(p_1-p_5)^2]^{-1}$$
$$\times [S(p_1,\epsilon^*(p_5),p_1-p_5,p_3)^{--} S(p_4,p_2)^{--} - S(p_4,p_3)^{--} S(p_1,\epsilon^*(p_5),p_1-p_5,p_2)^{--}] , \quad \text{(A8)}$$

$$m_c^{\bar{\nu}} = 2F \sin^2\theta_W [(p_2-p_4)^2 - M_W^2]^{-1} [(p_3+p_5)^2]^{-1}$$
$$\times [S(p_1,p_2)^{--} S(p_4,p_3+p_5,\epsilon^*(p_5),p_3)^{+}_{--} - S(p_4,p_2)^{--} S(p_1,p_3+p_5,\epsilon^*(p_5),p_3)^{+}_{--}] , \quad \text{(A9)}$$

$$m_d^{\bar{\nu}} = -F(-1+\tfrac{2}{3}\sin^2\theta_W)[(p_1-p_3)^2 - M_W^2]^{-1} [(p_4+p_5)^2]^{-1}$$
$$\times [S(p_1,p_3)^{--} S(p_4,\epsilon^*(p_5),p_4+p_5,p_2)^{--} - S(p_1,p_2)^{--} S(p_4,\epsilon^*(p_5),p_4+p_5,p_3)^{--}] , \quad \text{(A10)}$$

$$m_e^{\bar{\nu}} = -F(1-\tfrac{4}{3}\sin^2\theta_W)[(p_1-p_3)^2 - M_W^2]^{-1} [(p_2-p_5)^2]^{-1}$$
$$\times [S(p_1,p_3)^{--} S(p_4,p_2-p_5,\epsilon^*(p_5),p_2)^{+}_{--} - S(p_4,p_3)^{--} S(p_1,p_2-p_5,\epsilon^*(p_5),p_2)^{+}_{--}] . \quad \text{(A11)}$$

The matrix element squared is then given by

$$|m|^2=|m_a+m_b+m_c+m_d+m_e|^2 , \tag{A12}$$

which is evaluated numerically.

[1]K. Hagiwara, R. D. Peccei, D. Zeppenfeld, and K. Hikasa, Nucl. Phys. **B282**, 235 (1987).

[2]G. Couture and J. N. Ng, Z. Phys. C **32**, 579 (1986).

[3]K. O. Mikaelian, M. A. Samuel, and D. Sahdev, Phys. Rev. Lett. **43**, 746 (1979); R. W. Brown, D. Sahdev, and K. O. Mikaelian, Phys. Rev. D **20**, 1164 (1979).

[4]I. F. Ginsburg *et al.*, Nucl. Phys. **B228**, 285 (1983); K. O. Mikaelian, Phys. Rev. D **30**, 1115 (1984); G. Couture, S. Godfrey, and P. Kalyniak, *ibid.* **39**, 3239 (1989).

[5]For a discussion of the expected neutrino and muon fluxes at the SSC, see S. Loken and J. G. Morfin, in *Proceedings of the Summer Study on the Design and Utilization of the Superconducting Super Collider,* Snowmass, Colorado, 1984, edited by R. Donaldson and J. G. Morfin (Division of Particles and Fields of the APS, New York, 1985).

[6]R. Ruckl, DESY Report No. 88-191, 1988 (unpublished); G. Altarelli, B. Mele, and R. Ruckl, in *Proceedings of the CERN-ECFA workshop on Feasibility of Hadron Colliders in the LEP Tunnel,* Lausanne, Switzerland, 1984 (CERN Report No. 84-10, Geneva, 1984), p. 549; G. Altarelli and R. Ruckl, Nucl. Phys. **B262**, 204 (1985).

[7]R. W. Brown, L. B. Gordon, J. Smith, and K. O. Mikaelin, Phys. Rev. D **13**, 1856 (1976).

[8]G. Couture, J. N. Ng, J. Hewett, and T. Rizzo, Phys. Rev. D **36**, 859 (1987).

[9]G. Couture and J. N. Ng, Z. Phys. C **35**, 65 (1987).

[10]K. Hagiwara and D. Zeppenfeld, Nucl. Phys. **B274**, 1 (1986).

[11]E. Eichten, I. Hinchliffe, K. Lane, and C. Quigg, Rev. Mod. Phys. **56**, 579 (1984).

[12]C. Quigg, M. H. Reno, and T. P. Walker, Phys. Rev. Lett. **57**, 774 (1986).

[13]On the other hand, the cross section for $\mu^+N\rightarrow\mu^+Z^0X$ is much bigger since this is mainly a electromagnetic bremsstrahlung process, see Ref. 7.